



Research articles

Ar ion irradiation effect on the soft magnetic performance of Fe-based amorphous alloys

Qiang Luo^{a,b}, Xindu Fan^a, Baowei Miao^b, Baolong Shen^{a,c}, Jun Shen^{d,*}^a School of Materials Science and Engineering, Jiangsu Key Laboratory for Advanced Metallic Materials, Southeast University, Nanjing 211189, China^b School of Materials Science and Engineering, Tongji University, 4800 Caoan Road, Shanghai 201804, China^c Institute of Massive Amorphous Metal Science, China University of Mining and Technology, Xuzhou 221116, China^d College of Mechatronics and Control Engineering, Shenzhen University, Shenzhen 518060, China

A B S T R A C T

We investigate the effect of Ar ion irradiation on the microstructure and soft magnetic behaviors of $\text{Fe}_{80}\text{Co}_x\text{B}_{14-x}\text{Si}_2\text{P}_3\text{Cu}_1$ ($x = 0, 2, 4$) amorphous alloys by using X-ray diffraction (XRD), differential scanning calorimetry (DSC) and soft magnetic performance analysis. With increasing Co content, the alloy shows decreasing radiation resistance, i.e., more degree of nanocrystallization induced by irradiation. It is found that after irradiation with fluence of $\sim 9.0 \times 10^{14}$, the coercivity is reduced from 7.6 A/m to 7.0 A/m, but increases again with further increase of irradiation fluence due to the formation of larger nanosized α -Fe(Co) grains. And with increasing irradiation fluence, the saturation magnetic flux density first decreases slightly from 1.65 T to 1.64 T, and then increases gradually to 1.68 T. Further, the core loss and effective magnetic conductivity were tuned obviously by irradiation, which has been discussed in term of stress relaxation and nanocrystallization.

1. Introduction

Soft magnetic amorphous and related nanocrystalline alloys with excellent magnetic properties, such as high saturation magnetic flux density (B_s), low magnetic core loss (W), low coercivity (H_c) and high permeability (μ), have exhibited promising application future in various energy saving required electric devices [1–10]. In fact, three families of alloy systems, Finemet, Nanoperm, and Hitperm have been commercially used due to their excellent magnetic performances [10–13]. Nevertheless, the improvement of soft magnetic performances of amorphous/nanocrystalline alloys by material design and various post treatments is continuously attracting world-wide research interest due to both scientific and technological reasons. Especially, many studies were devoted to synthesis of nanocrystalline structure with a high concentration of uniformly distributed single-phase nanocrystals in the amorphous matrix by thermal annealing to pursue optimal magnetic performance [1–8]. Note that crystallization of amorphous alloys can also occur by non-thermal processes such as deformation and irradiation (electron, neutron and other ions) [14–18]. Electron irradiation is often used to engender amorphization of crystalline phases or nanocrystallization of amorphous solids. And obvious differences in crystallization process have been observed between thermal annealing and irradiation methods [18,19]. In addition, ion irradiation has used to modify magnetic properties such as magnetic transition temperature, magnetic permeability and coercivity [14–17,20]. Kim et al., reported that initial permeability increased after neutron irradiation (up to 10^{16}

/cm² fluence), but the H_c and B_s remained almost unchanged [17]. In the $\text{Fe}_{80}\text{Cr}_2\text{Si}_4\text{B}_{14}$ sample, it was found that neutron irradiation increased the coercive force and decreased the saturation magnetization [16]. Le et al., observed a large enhancement of the giant magnetoimpedance effect in N and Xe ion-irradiated $\text{Co}_{69}\text{Fe}_{4.5}\text{Al}_{1.5}\text{Si}_{10}\text{B}_{15}$ amorphous alloys, which was suggested to result from the enhancement of permeability [21]. Peng et al., reported that Ar ion irradiation in short time only led to structure relaxation and enhanced the permeability of $\text{Fe}_{73.5}\text{Si}_{13.5}\text{B}_9\text{Nb}_3\text{Cu}_1$ amorphous alloy; however, further increasing the irradiation time led to crystallization, increased residual stress and magnetic anisotropy, and thus lower permeability [22]. Škorvánek et al., observed a deterioration of the soft magnetic behavior in a Fe-based amorphous alloy by neutron irradiation, and found that the defect structures induced by irradiation could recover by annealing [23]. In addition, there are also some investigations on the influence of irradiation on radiation-resistance and mechanical performances of amorphous alloys [24], due to the application prospects of these alloys as radiation-, wear- and corrosion-resistant materials.

At present, there have very few systematic studies on the response of soft magnetic performance with ion irradiation in Fe-based amorphous alloys. A few publications only investigated the change of one or two magnetic parameters after irradiation in these alloys [14–17]. In present study, we explored systematically the influence of Ar ion irradiation on the structure and soft magnetic behaviors of $\text{Fe}_{80}\text{Co}_x\text{B}_{14-x}\text{Si}_2\text{P}_3\text{Cu}_1$ ($x = 0, 2, 4$) amorphous alloys. The changes of B_s , μ , W and H_c with Ar ion irradiation fluences of 9.0×10^{14} , 6.0×10^{15} and

* Corresponding author.

E-mail address: junshen@szu.edu.cn (J. Shen).

$2.0 \times 10^{16} / \text{cm}^2$ have been discussed in term of the irradiation-induced structure relaxation and nanocrystallization. Improvement of magnetic softness has been obtained after proper Ar ion irradiation, but deterioration after excessive irradiation, and the possible reasons are discussed.

2. Experiment

Alloy ingots with compositions of $\text{Fe}_{80}\text{Co}_x\text{B}_{14-x}\text{Si}_2\text{P}_3\text{Cu}_1$ ($x = 0, 2, 4$) were remelted by induction melting, and then ribbons with thickness of $\sim 22 \mu\text{m}$ were fabricated from the ingots by melt spinning method. Ar ion irradiation with energy of 170 keV was carried out on an ion irradiation system in a vacuum of $\sim 1.33 \times 10^{-2}$ Pa. Three different fluences of 9.0×10^{14} , 6.0×10^{15} and $2.0 \times 10^{16} / \text{cm}^2$ were obtained, and the samples irradiated under these conditions were marked as I14, I15 and I16, respectively. Microstructure of the samples was checked by X-ray diffraction (XRD, Cu $K\alpha$ radiation). The crystallization event of the as-spun and irradiated samples was analyzed by using differential scanning calorimetry (DSC) method at a heating rate of $40 \text{ }^\circ\text{C}/\text{min}$ under argon flow. B_s was determined by a vibrating sample magnetometer (VSM) under a field of 800 kA/m. The permeability at different frequencies was obtained by an impedance analyzer. H_c and W were determined by DC and AC B-H analyzer, respectively.

3. Results and discussion

Fig. 1(a) presents the XRD patterns of as-spun and irradiated $\text{Fe}_{80}\text{Co}_2\text{B}_{12}\text{Si}_2\text{P}_3\text{Cu}_1$. All samples were examined on the free surface. Only a broad halo and no obvious diffraction peak can be observed within the resolution limit of XRD for the as-spun and I14 samples, showing their almost fully amorphous structure (similar results for other two as-spun ribbons with $x = 0$ and 4). Nevertheless, obvious diffraction peak can be observed for the I15 and I16 samples, whose intensity increases with increasing irradiation fluence. And the average sizes are determined to be 14 nm and 60 nm roughly, for the irradiated I15 and I16 samples, respectively. Note that here the crystallization-phase ratio and grain size are determined just for the surface layer of the ribbons. This change of XRD pattern indicates obviously the increasing content of the crystallization phase with increasing irradiation time, which can be understood as follows. Usually the crystallization of amorphous alloy contains the following two related processes: (1) the formation and growth of related precursor clusters and (2) the nucleation and growth of crystals. And both the formation and growth of precursor clusters and crystals take time. For the FeCoBSiPCu alloy system [10], it was reported that some preexisted clusters and even a few crystal nuclei existed in the as-spun ribbon, although they cannot be detected by XRD. During the ion irradiation process, the energy of Ar ion can convert into heat partly, and the momentum into force partly. The resulting anisotropy stress and heating effects render the structure change of the Fe-based alloy. During irradiation with small fluence (for the I14 sample), the atomic rearrangement occurs only over a short range, which only leads to the growth of precursor clusters and pre-existed crystal nuclei, the formation of some new ordered clusters, and eliminates some defects in the as-spun sample (accompanying stress/structural relaxation). As the irradiation fluence increases, more heat transferred from the energy of the Ar ions accumulates to increase the temperature, which leads to nanocrystallization through long range atomic rearrangement. By comparing the three alloys, it can be found that the $x = 0$ sample has the strongest irradiation-resistance ability (since it remains always amorphous after irradiation), and Co addition impairs this resistance ability as seen from the XRD patterns of all the irradiated samples (Fig. 1(b)).

The crystallization of the surface layer of the samples induced by Ar irradiation can be illustrated further from the DSC curves. Fig. 2 shows the thermal properties of the as-spun and irradiated $\text{Fe}_{80}\text{Co}_2\text{B}_{12}\text{Si}_2\text{P}_3\text{Cu}_1$ samples, all of which exhibit two large exothermic

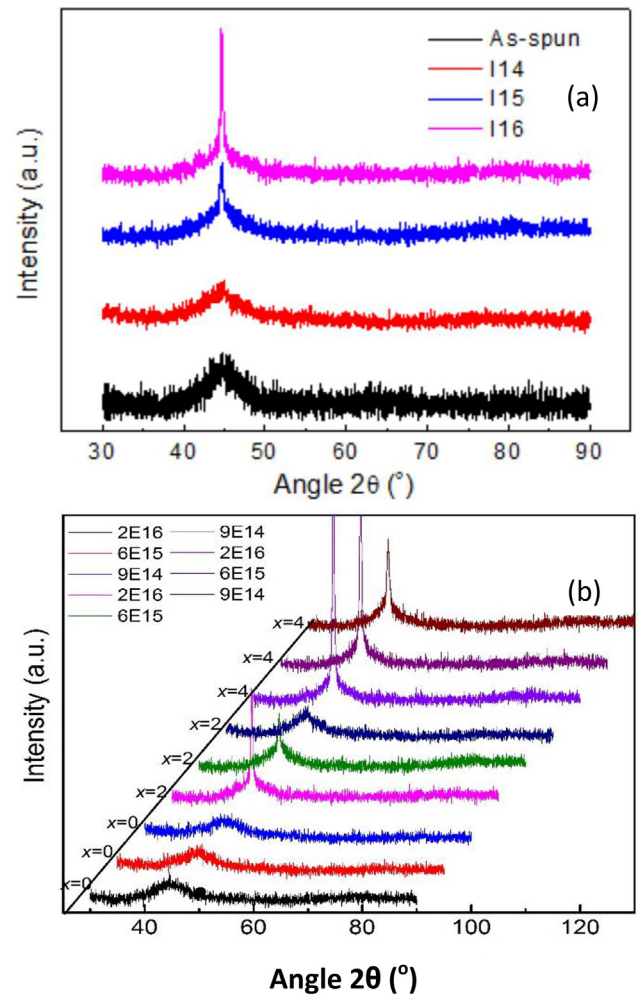


Fig. 1. (a) XRD patterns of the as-spun and irradiated $\text{Fe}_{80}\text{Co}_2\text{B}_{12}\text{Si}_2\text{P}_3\text{Cu}_1$ samples. (b) XRD patterns of all the irradiated samples.

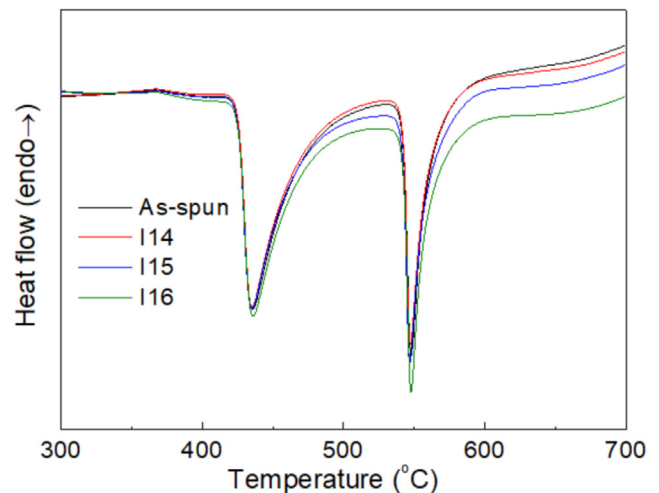


Fig. 2. DSC curves of the as-spun and irradiated samples.

peaks due to crystallization. From the curve, the onset crystallization temperature T_x can be determined to be $422 \text{ }^\circ\text{C}$ for the as-spun $\text{Fe}_{80}\text{Co}_2\text{B}_{12}\text{Si}_2\text{P}_3\text{Cu}_1$. The amorphous alloy is partially transformed to nanocrystalline $\alpha\text{-Fe}(\text{Co})$ phase during the first stage crystallization, and completes the crystallization process in the secondary stage. Note that the crystallization temperatures of all the samples under different

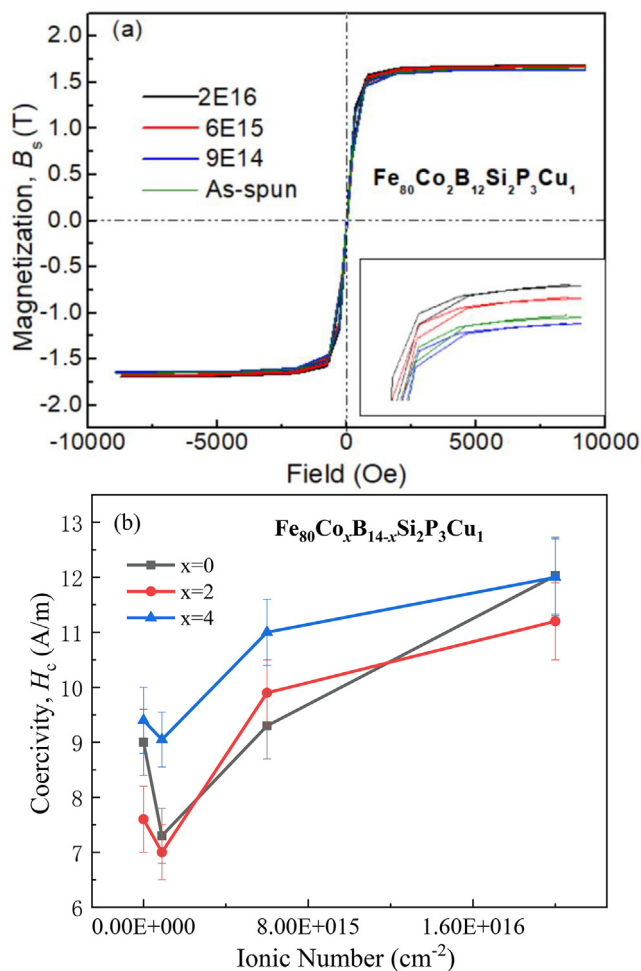


Fig. 3. (a) Hysteresis curves of the as-spun and irradiated samples, the inset shows the enlarged part of saturation. (b) Variation of H_c with irradiation fluence for the three compositions.

fluences remain almost the same. Nevertheless, the crystallization enthalpy changes obviously after irradiation as seen from Fig. 2, implying different degrees of nanocrystallization in the irradiated samples with different fluences.

The B-H curves of the as-spun and irradiated samples are shown in Fig. 3 for $\text{Fe}_{80}\text{Co}_2\text{B}_{12}\text{Si}_2\text{P}_3\text{Cu}_1$ as an example, from which the B_s can be determined to be 1.65, 1.64, 1.67, 1.68 T, for the as-spun, irradiated I14, I15, I16 samples, respectively. It is known that the magnetic properties such as H_c and B_s are sensitive to the local structural features of solids like strain, grain size, defects etc. As discussed above, during the initial stage of bombardment of Ar ion, atoms of the sample can move over a short limited range driven by the force resulting from the elastic and inelastic collision with energetic Ar ions, which causes local structure relaxation and atomic rearrangements. With increasing irradiation time, the atoms can move over a longer range due to the force effect from the ions (the movement gets assistance from the thermal effect of irradiation), which leads to formation and growth of the Fe-Fe clusters and finally crystallization. It has been known that uniform precipitation of nanometer-scale *bcc*-Fe (α -Fe) grains may favor soft magnetic performance of the Fe-based alloys [1,2]. In addition, the Co addition in the sample help to obtain a higher B_s , considering that binary Fe-Co alloys have higher B_s than pure Fe [25]. The profitable effect of proper Co addition on the soft magnetic performance in Fe-based amorphous and (nano)crystalline alloys was observed in many systems [26–28]. Therefore, the enhancement of B_s with increasing irradiation fluence (above 9.0×10^{14}) in present alloy system may be

due to the increase of content and volume fraction of nanocrystalline α -Fe(Co) phase with increasing fluence as indicated from the change of α -Fe(Co) diffraction peak feature (Fig. 1). In addition, the slightly decrease of B_s for the I14 sample may be related to the force and thermal effects of irradiation, which change the local atomic configuration and decrease the exchange interaction. At present, the detailed mechanism is not clear, which needs more investigations in the future.

The H_c is sensitive to the Ar ion irradiation and shows a non-monotonic behavior for all the compositions, which first decreases after short-time irradiation (I14), and then increases with further increasing influence. The initial decrease of H_c may be due to stress relaxation and fine α -Fe(Co) cluster formation. The as-spun ribbon exhibits magnetic anisotropy either in plane or out of plane, which is magnetostrictive in nature. During the short time irradiation, internal stresses generated during fabrication can be relaxed accompanying the atomic rearrangement (note that additional residual stress can appear as the irradiation time increases). The initial stress relaxation may lead to annihilation of the quasi-defects (like quasi-dislocation dipoles and free/anti-free volume) in the glass, which reduces long-range stress fields pinning the domain walls [1–4]. The fine α -Fe(Co) cluster formation further makes for magnetic softness. Long-time irradiation results in formation and growth of the nanocrystals, which could be the main reason for the increase of H_c above the fluence of 9.0×10^{14} . In addition, long time ion bombardment can produce compressive force, and crystallization under anisotropic stress tends to increase magnetic anisotropy. This resulted magnetocrystalline anisotropy can overcome the decrease of quenched-in magnetoelastic induced magnetic anisotropy after long-time irradiation with fluences of 6.0×10^{15} and 2.0×10^{16} , which can also increase H_c . Similar variation trend of H_c with irradiation influence has also been observed in other two compositions as seen from Fig. 3 (b). Considering that the $x = 2$ sample has the lowest H_c , in the following we focus on this sample. Other two compositions show similar response to irradiation with this $x = 2$ sample.

The frequency dependence of μ is shown in Fig. 4(a) for the as-spun and irradiated $\text{Fe}_{80}\text{Co}_2\text{B}_{12}\text{Si}_2\text{P}_3\text{Cu}_1$ (B12) samples and in Fig. 4(b-c) for $\text{Fe}_{80}\text{Co}_4\text{B}_{10}\text{Si}_2\text{P}_3\text{Cu}_1$ (B10) and $\text{Fe}_{80}\text{B}_{14}\text{Si}_2\text{P}_3\text{Cu}_1$ (B14) samples. Generally, Ar irradiation leads to obvious increase of the μ compared with the as-spun sample (Fig. 4(a)), which might be due to the α -Fe(Co) cluster formation and relaxation effect. During irradiation, local structural relaxation occurs, which can decrease the stress-induced anisotropy and eliminate the liquid-like sites such as the free volume, possibly leading to the decrease of μ . At the same time, irradiation induced nanocrystallization can further reduce magnetic anisotropy when the magnetocrystalline anisotropy does not overcome the decrease of magnetoelastic induced magnetic anisotropy, which also may increase the magnetic conductivity. However, after irradiation for around some critical fluence, magnetocrystalline anisotropy may play a significant role and overcome the decrease of magnetoelastic induced magnetic anisotropy, which may decrease the μ (as seen in Fig. 4). Magnetic conductivity at 1 kHz, is determined to be 2440, 5640, 5270, 4870, for the as-spun, I14, I15 and I16 samples, respectively. Among the three irradiated samples, the I14 sample has the highest magnetic conductivity between 1000 and 8600 Hz, while above 8600 Hz, the I15 sample has. Present results indicate that the proper nanocrystallization can improve the high frequency performance of the alloys. Fig. 5 shows magnetic core loss under different fields for the irradiated $\text{Fe}_{80}\text{Co}_2\text{B}_{12}\text{Si}_2\text{P}_3\text{Cu}_1$ samples at 50 Hz. All the samples have relatively low W , which increases with increasing field. Relatively low W at high B_m of ~ 1.5 T is of significance for saving energy loss in many magnetic applications. The I14 and I15 samples show almost the same W especially below 1.1 T, above which larger W is observed for the I15 sample. And the I16 sample has the largest W values in the whole field range, which might be associated with the largest grain size of α -Fe(Co) with larger magnetocrystalline anisotropy in this sample.

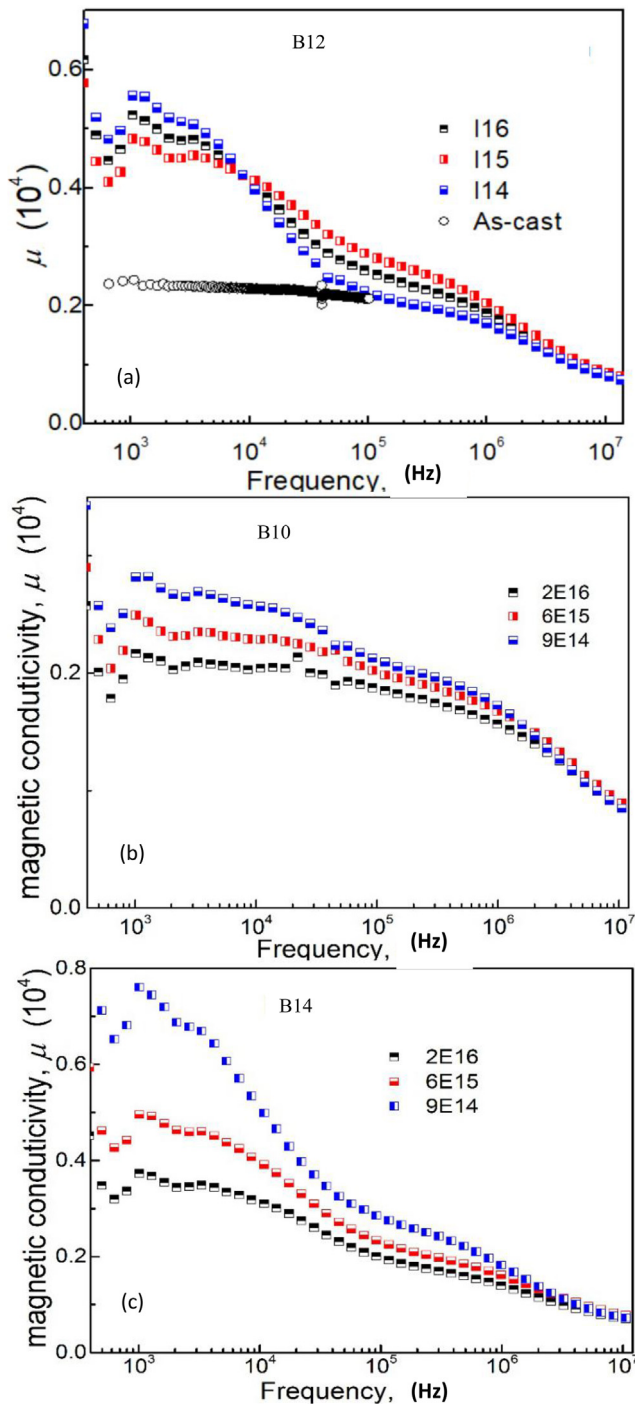


Fig. 4. (a) Dependence of magnetic conductivity on frequency for the as-spun and irradiated $\text{Fe}_{80}\text{Co}_x\text{B}_{14-x}\text{Si}_2\text{P}_3\text{Cu}_1$ (B12); (b) and (c) for the irradiated $\text{Fe}_{80}\text{Co}_4\text{B}_{10}\text{Si}_2\text{P}_3\text{Cu}_1$ (B10) and $\text{Fe}_{80}\text{B}_{14}\text{Si}_2\text{P}_3\text{Cu}_1$ (B14) samples, respectively.

4. Summary

In conclusion, effects of Ar ion irradiation with different fluences on the structure and magnetic behaviors of $\text{Fe}_{80}\text{Co}_x\text{B}_{14-x}\text{Si}_2\text{P}_3\text{Cu}_1$ ($x = 0, 2, 4$) amorphous alloys have been investigated. Irradiation can induce relaxation and nanocrystalline $\alpha\text{-Fe}(\text{Co})$ formation of the amorphous alloys, and alter the residual stress and magnetic anisotropy. Ar ion irradiation with a relatively low fluence of 9.0×10^{14} decreases H_c and increases μ at 1 kHz obviously with only a slight reduction of B_s . With further increase of the fluence, irradiation deteriorates the magnetic softness, decreases μ , but enhances B_s , which is mainly due to the

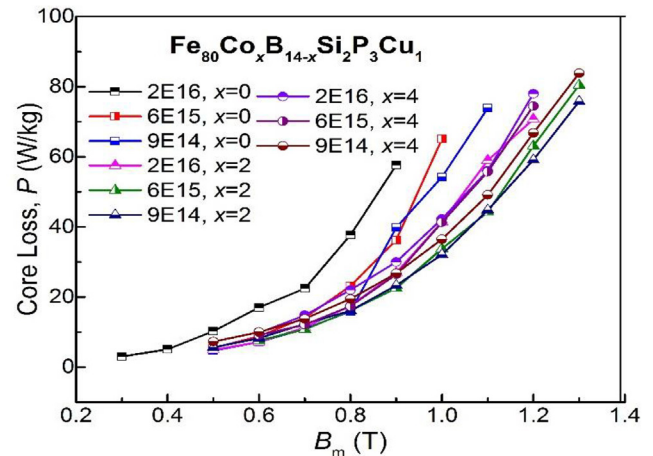


Fig. 5. Dependence of magnetic core loss (W) on the induction for the irradiated alloys.

relatively higher volume fraction of crystals with larger grain sizes formed during long-time irradiation and the altered magnetic anisotropy in the alloys. Therefore, present work demonstrates that ion irradiation can be applied for improvement of soft magnetic performances in Fe-based amorphous and nanocrystalline alloys.

5. Author statement

Qiang Luo and Jun Shen designed experiments; Qiang Luo and Baowei Miao carried out experiments; all authors analyzed experimental results. Qiang Luo wrote the manuscript with the contributions from all other co-authors.

Declaration of Competing Interest

The authors declare that they have no known competing financial interests or personal relationships that could have appeared to influence the work reported in this paper.

Acknowledgments

This work is financially supported by the National Key Research and Development Plan of China (Grant No. 2016YFB0300502) and the National Science Foundation of China (Grant Nos. 51971061 and 51601130).

Appendix A. Supplementary data

Supplementary data to this article can be found online at <https://doi.org/10.1016/j.jmmm.2020.166962>.

References

- [1] G. Herzer, *Acta Mater.* 61 (2013) 718.
- [2] H. Matsumoto, A. Urata, Y. Yamada, A. Inoue, *J. Alloys Compd.* 509 (2011) S193.
- [3] F.L. Kong, C.T. Chang, A. Inoue, E. Shalaaan, F. Al-Marzouki, *J. Alloys Compd.* 615 (2014) 163.
- [4] C.L. Zhao, A.D. Wang, A.N. He, S.Q. Yue, C.T. Chang, X.M. Wang, *J. Alloys Compd.* 659 (2016) 193.
- [5] A. Inoue, Y. Shinohara, J.S. Gook, *Mater. Trans. JIM* 36 (1995) 1427.
- [6] M. Ohta, Y. Yoshizawa, *J. Magn. Magn. Mater.* 320 (2008) e750.
- [7] M.A. Willard, D.E. Laughlin, M.E. McHenry, D. Thoma, K. Sickafus, J.O. Cross, V.G. Harris, *J. Appl. Phys.* 84 (1998) 6773.
- [8] A. Makino, H. Men, K. Yubuta, T. Kubota, *J. Appl. Phys.* 105 (2009) 013922.
- [9] X.D. Fan, H. Men, A.B. Ma, B.L. Shen, *J. Magn. Magn. Mater.* 326 (2013) 22.
- [10] K. Takenaka, A.D. Setyawan, Y. Zhang, P. Sharma, N. Nishiyama, A. Makino, *Mater. Trans. JIM* 56 (2015) 372.
- [11] A. Makino, T. Bitoh, A. Inoue, T. Masumoto, *Scr. Mater.* 48 (2003) 869.
- [12] M.E. McHenry, F. Johnson, H. Okumura, T. Ohkubo, V.R.V. Ramanan,

- D.E. Laughlin, *Scr. Mater.* 48 (2003) 881.
- [13] Y. Yoshizawa, K. Yamauchi, T. Yamane, H. Sugihara, *J. Appl. Phys.* 64 (1988) 6047.
- [14] P.J. Grundy, G.A. Jones, S.F.H. Parker, *IEEE Trans. Magn.* 19 (1983) 1913.
- [15] R.D. Brown, J.R. Cost, J.T. Stanley, *J. Appl. Phys.* 55 (1984) 1754.
- [16] M. Miglierini, I. Škorvánek, *Mater. Sci. Eng. A* 147 (1991) 101.
- [17] H.C. Kim, S.C. Yu, C.G. Kim, H.S. Han, W.K. Cho, *J. Magn. Magn. Mater.* 215–216 (2000) 355.
- [18] A. Nino, T. Nagase, Y. Umakoshi, *Mater. Trans.* 46 (2005) 181.
- [19] W. Qin, T. Nagase, Y. Umakoshi, *Acta Mater.* 57 (2009) 1300.
- [20] H.C. Kim, S.C. Yu, C.G. Kim, H.S. Han, W.K. Cho, D.H. Kim, *J. Appl. Phys.* 87 (2000) 7115.
- [21] A.T. Le, et al., *Mater. Sci. Eng. B* 166 (2010) 89.
- [22] K. Peng, L. Tang, Y. Wu, *J. Magn. Magn. Mater.* 460 (2018) 297.
- [23] I. Škorvánek, R. Gerling, *J. Appl. Phys.* 72 (1992) 3417.
- [24] W.D. Luo, B. Yanga, G.L. Chen, *Scr. Mater.* 64 (2011) 625.
- [25] C. Kuhrt, L. Schultz, *J. Appl. Phys.* 71 (1992) 1896.
- [26] F. Wang, et al., *J. Alloys Compd.* 723 (2017) 376.
- [27] F. Wang, A. Inoue, Y. Han, F.L. Kong, S.L. Zhu, E. Shalaan, F. Al-Marzouki, A. Obaid, *J. Alloys Compd.* 711 (2017) 132.
- [28] Y. Han, J. Ding, F.L. Kong, A. Inoue, S.L. Zhu, Z. Wang, E. Shalaan, F. Al-Marzouki, *J. Alloys Compd.* 691 (2017) 364.